processes

MDPI

*Review*

# A Review of In Situ Pyrolysis Technologies, Kinetics and Influencing Factors for Oil Shale Based on Thermogravimetric Analysis

**Yuanqing Wang [1,2], Zhilin Tian [3], Qi Xia [3], Manlai Zhang [3,*], Zijun Wu [3], Heng Liu [3] and Junwei Sun [3]**

[1] State Center for Research and Development of Oil Shale Exploitation, State Key Laboratory of Shale Oil and Effective Development, Beijing 100083, China
[2] Petroleum Exploration and Production Research Institute of SINOPEC, Beijing 100000, China
[3] School of Mechanical Engineering, Yangtze University, Jingzhou 451199, China
* Correspondence: zhmanlai@163.com

**Abstract**

As a vital unconventional oil and gas resource, the efficient exploitation of oil shale relies on breakthroughs in pyrolysis conversion technologies. Based on thermogravimetric analysis and related thermal analysis studies, this paper systematically reviews the technologies, kinetics and influencing factors of oil shale pyrolysis, following the framework of "rock properties—pyrolysis technologies and conditions—kinetic characterization—reaction and product formation—engineering factors and responses." First, typical oil shale deposits, including the Green River (USA), Fushun and Maoming (China), Estonian Kukersite and Brazilian Irati, are compared in terms of kerogen type, mineral composition, oil yield and pyrolysis kinetic parameters. Rock properties are shown to be the fundamental determinant of pyrolysis behaviour. Second, the characteristics of surface retorting (gaseous/solid heat carriers) and in situ pyrolysis (conduction, convection, radiation and reaction-heat heating) are summarized, emphasizing that experimental observations from surface retorting cannot be directly extrapolated to the in situ scale. Third, the applicable conditions and limitations of the Arrhenius, Coats–Redfern, Friedman, FWO and KAS methods are systematically compared. Isoconversional methods (Friedman, FWO and KAS) are shown to effectively capture the dynamic evolution of activation energy with conversion degree, making them more suitable for characterizing the multi-stage and heterogeneous nature of oil shale pyrolysis. Furthermore, hydrocarbon generation pathways and product distribution patterns are analyzed from the perspectives of pyrolysis staging, primary kerogen conversion and secondary cracking. Secondary cracking is identified as the critical process governing oil composition under high-temperature conditions. Finally, the effects of particle size, heating rate, pyrolysis temperature and pressure on product yield and composition are discussed. Future research should advance from "kinetic parameter calculation" toward "product yield prediction," providing theoretical references for multi-field coupling simulation and engineering-parameter optimization of in situ oil shale pyrolysis.

**Keywords:** oil shale; pyrolysis; in situ conversion; kinetic model; product distribution; influencing factors

Check for updates

Academic Editors: Shu Tao, Shida Chen, Zhengguang Zhang, Yu Song and Qiong Wang

Received: 13 August 2026
Revised: 20 September 2026
Accepted: 22 September 2026
Published: 27 September 2026

**Copyright:** © 2026 by the authors. Licensee MDPI, Basel, Switzerland. This article is an open access article distributed under the terms and conditions of the Creative Commons Attribution (CC BY) license.

## 1. Introduction

With the continuous growth of global energy demand and the increasing difficulty in exploiting conventional oil gas resources, unconventional hydrocarbon resources have

attracted growing attention within the energy supply system. Oil shale is a sedimentary rock rich in solid organic matter, which is mostly hosted within the mineral matrix in the form of kerogen [1,2]. Unlike conventional petroleum, organic matter in oil shale cannot be directly recovered by conventional oil-production methods. Heating is required to trigger kerogen thermal cracking, yielding liquid hydrocarbons, gaseous hydrocarbons and solid residues. Accordingly, pyrolysis conversion constitutes the core procedure for effective utilization of oil shale resources [3–6].

Conventional surface retorting technologies require mining, crushing, transportation and above-ground heating processes, which are associated with high energy consumption, environmental disturbance and challenges in waste management. In contrast, in situ pyrolysis directly introduces heat into underground formations to establish thermal conversion zones, allowing hydrocarbons generated from kerogen transformation to be recovered through production wells. Consequently, in situ conversion technology has emerged as a promising approach for improving resource utilization efficiency and reducing environmental impacts [7,8]. A wide range of techniques, including thermogravimetric analysis (TGA), fixed-bed pyrolysis, retorting experiments and numerical simulation, have been employed to investigate oil shale pyrolysis behaviours [9]. Among them, TGA is widely applied because it provides continuous measurements of mass variation during heating and enables the determination of kinetic parameters such as activation energy and reaction order [10–14].

Despite extensive investigations, several challenges remain in linking laboratory-scale observations with engineering-scale applications. Laboratory experiments provide fundamental insights into pyrolysis mechanisms and kinetic characteristics, but reservoir-scale processes involve complex interactions among heat transfer, fluid migration, phase change, pore evolution and hydrocarbon production [15–17]. Therefore, an integrated understanding of oil shale properties, pyrolysis conditions, reaction mechanisms, product formation, kinetic characterization and engineering-scale responses is required. This review systematically summarizes recent progress in oil shale pyrolysis research following the framework of "oil shale properties—pyrolysis conditions—reaction processes—product formation—kinetic characterization—engineering-scale responses" Figure 1. The relationships among geological characteristics, thermal conversion behaviour, kinetic models and engineering applications are discussed to provide insights for the optimization of in situ pyrolysis technologies.

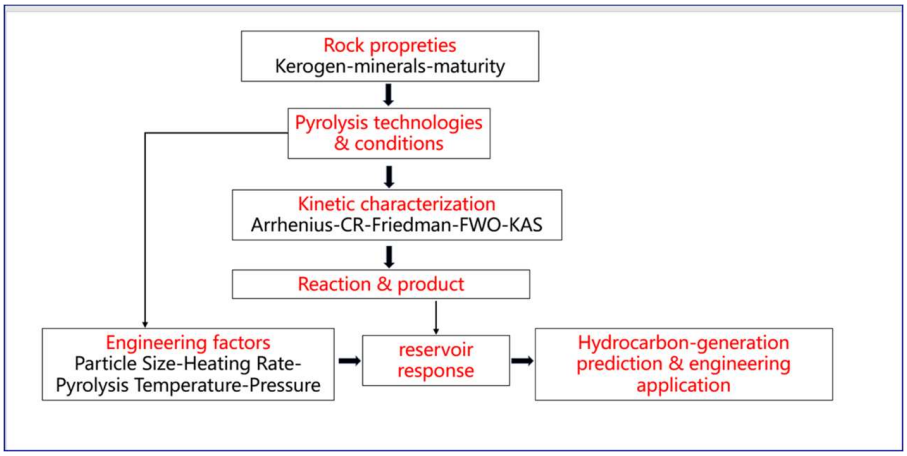


**Figure 1.** Review framework linking rock properties, pyrolysis conditions, kinetics, reaction/product formation and engineering response.

## 2. Properties of Oil Shale and Pyrolysis Technologies

### 2.1. Basic Properties of Oil Shale in Different Regions

Significant differences exist among oil shales from different regions in terms of sedimentary environment, organic matter source, kerogen type, mineral composition and thermal maturity. Accordingly, their pyrolysis onset temperature, reaction rate, oil gas yield and product composition do not follow a universal rule. Previous studies have demonstrated that distinct pyrolysis kinetics and product distribution characteristics can still be observed for different oil shales even under identical pyrolysis temperature and heating conditions. Therefore, it is necessary to clarify the petrological and organic–geochemical basis of the research objects prior to discussing oil shale pyrolysis mechanisms.

"To avoid over-generalizing pyrolysis laws derived from one specific deposit, it is necessary to analyze the vast heterogeneity of global oil shale reserves. Studies have deeply investigated world-renowned deposits such as the Green River oil shale in the USA [18–20], which is famous for its Type-I kerogen, and the Kukersite oil shale in Estonia [21] and Irati oil shale in Brazil [5], which offer unique algal-derived characteristics. In China, extensive thermal and kinetic evaluations have been conducted on diverse regional deposits, including Fushun oil shale [22], Jimsar oil shale [23,24], Wangqing oil shale [25] and organic-rich formations in the northern Songliao Basin [26]. To further broaden this perspective, recent analytical kinetics research has also characterized shales from the Moroccan Rif [10,27], Jordanian deposits like Omari [28,29], Turkish shales [2], the Democratic Republic of the Congo [30] and North Korea [31,32]. Comparative analysis of these diverse cases provides a robust theoretical foundation encompassing varied kerogen architectures and mineral assemblages."

Green River oil shale is primarily composed of organic-rich lacustrine deposits. Investigations confirm that its organic matter is dominated by Type-I kerogen with strong hydrocarbon generation potential. It has long served as a key target for in situ pyrolysis research. Pyrolysis experiments on Green River oil shale cover conventional retorting, semi-open systems and in situ conversion scenarios, making it a representative case bridging laboratory-scale pyrolysis and in situ pyrolysis studies.

Fushun oil shale possesses solid research foundations on mineral–organic matter interactions. Its principal mineral phases include quartz, calcite, illite and montmorillonite. Strong structural associations occur between minerals and kerogen; mineral assemblages can modify kerogen pyrolysis pathways and product release behaviours. Multiple analytical techniques such as TG-FTIR, Py-GC/MS, XRD and structural characterization have been applied to resolve its pyrolysis kinetics, gas evolution patterns and reaction pathways. Hence, Fushun oil shale is suitable as a typical case for unravelling the relationships among "mineral composition–kerogen structure–pyrolysis behaviour".

Maoming oil shale displays typical lacustrine organic matter signatures. Its samples feature high organic matter abundance, with TOC values ranging approximately from 16% to 23% in selected specimens. The kerogen is mainly Type I or transitional Type I–II at low thermal maturity. Clay minerals and quartz constitute its dominant mineral fractions. Thermal maturation experiments and $^{13}$C-NMR analyses reveal systematic variations in aliphatic and aromatic moieties within kerogen during thermal evolution, which directly govern the formation of liquid hydrocarbons, gaseous hydrocarbons and heavy-end products.

Estonian Kukersite oil shale shows prominent regional traits. Its organic matter is predominantly algal-originated, with highly diagnostic ratios between mineral matrix and kerogen. Kukersite kerogen contains abundant aliphatic structures. During pyrolysis, continuous transformation proceeds from kerogen to pyrobitumen, followed by further conversion of pyrobitumen into shale oil and gas. Accordingly, Kukersite oil shale is of great significance for exploring intermediate-product-controlled pyrolysis mechanisms.

Brazilian Irati oil shale also provides valuable comparative insights. Organic–geochemical evidence indicates that Irati oil shale contains algal-related Type I kerogen at low thermal maturity; its mineral matrix consists mainly of clay minerals, carbonates and pyrite. Kinetic studies on Irati oil shale demonstrate that apparent activation energy varies with conversion degree, suggesting multi-stage and heterogeneous pyrolysis characteristics.

Consequently, this work does not aim to construct a simple "location parameter" database based on the five oil shale deposits. By using differentiated typical cases, this paper establishes the linkage among "rock composition–kerogen structure–pyrolysis kinetics–product generation", laying a foundation for subsequent analysis of controlling factors governing oil shale pyrolysis behaviours.

### *2.2. Effects of Kerogen, Mineral Composition and Maturity on Pyrolysis*

Pyrolysis behaviour of oil shale is primarily governed by organic matter properties. Kerogen type, molecular structure and thermal maturity determine the initial thermal stability and hydrocarbon generation potential of organic matter. Kerogens of different types exhibit distinct H/C and O/C atomic ratios, as well as varied proportions of aliphatic moieties, aromatic moieties and heteroatom-containing functional groups, which result in divergent pyrolysis reactivity and product composition under identical thermal conditions. Taking Maoming oil shale as an example, Rock-Eval pyrolysis, elemental analysis and $^{13}$C-NMR measurements demonstrate that its Type I kerogen is rich in aliphatic structures. As thermal maturity increases, aliphatic fractions gradually decrease while aromatic components grow, accompanied by shifts in the relative yields of liquid and gaseous hydrocarbons. This indicates that kerogen structure not only controls the onset of pyrolysis but also governs product partitioning during primary pyrolysis and subsequent secondary cracking.

Thermal maturity further dictates the residual fraction of reactive structural units within kerogen. For low-maturity oil shale, kerogen retains abundant aliphatic structures with high hydrocarbon-generating capacity, enabling substantial organic matter conversion during pyrolysis. As maturity rises, certain reactive moieties are consumed during geological evolution, and the remaining organic matter becomes more thermally stable. Accordingly, when comparing pyrolysis results of oil shales from different regions, pyrolysis extent cannot be judged by final temperature alone; initial thermal maturity and kerogen structural discrepancies must also be considered. Organic–geochemical investigations on Irati oil shale reveal its Type I kerogen and low thermal maturity, which partially account for its considerable pyrolysis potential.

Mineral composition affects the pyrolysis process through both physical and chemical pathways. Detailed mineralogical characterizations indicate that inherent minerals such as silicates, carbonates, and clay not only alter the thermal conductivity of the matrix but also actively adsorb or catalyze intermediate organic products [27,33]. Furthermore, studies on specific shales (e.g., Huadian) demonstrate that the presence of transition metal salts can function as catalysts, significantly modifying secondary reaction pathways [8,34]. Mechanistic reviews further confirm that minerals are not merely inert matrices but critical participants in pyrolysis [35].

Mineral effects also complicate the interpretation of thermal analysis profiles. At high temperatures, oil shale undergoes not only kerogen decomposition but also carbonate decomposition, clay mineral dehydration and other inorganic transformations. Consequently, mass loss peaks in TG/DTG curves cannot be fully attributed to kerogen breakdown. Neglecting mineral-driven reactions may introduce errors in the estimation of activation energy, reaction order and pyrolysis stage division. This highlights the necessity of parallel pyrolysis tests using raw oil shale samples and demineralized kerogen.

Concurrently, the rock's architecture controls fluid expulsion. As kerogen thermally decomposes and releases volatile species, the internal pore structures evolve remarkably. Advanced microstructural imaging techniques (e.g., NMR, FESEM, TG-FTIR-MS) have proven that initially tight shale matrices undergo massive pore and fracture generation during heating, which fundamentally improves the diffusion and seepage conditions for the reaction products [36–39].

Therefore, oil shale pyrolysis should not be oversimplified as a single "kerogen thermal decomposition" process. Instead, it represents a coupled process integrating kerogen structural rearrangement, mineral effects, pore evolution and heat-volatile transport. This is particularly critical for in situ pyrolysis: pyrolysis reactions reshape porosity and permeability, and such pore structure variations in turn influence subsequent heat and hydrocarbon migration, establishing strong thermal reaction–seepage coupling.

### *2.3. Classification of Domestic and International Oil Shale Kinetic Methods*

In this paper, typical oil shale areas at home and abroad are classified according to different pyrolysis kinetic models and methods such as Coats–Redfern, Arrhenius, Friedman, FWO and KAS.

Table 1 provides a detailed classification of kinetic methods. The pyrolysis process of Huadian, Maoming and Fushun oil shales is simple, with concentrated reactions and clear reaction orders. The Coats–Redfern method eliminates the influence of heating rate through integration, and the Arrhenius method directly correlates temperature with reaction rate. The pyrolysis of Longkou, Green River and Liushuhe oil shales includes multiple different stages. When the Friedman method is used, there is no need to assume the reaction order, and the activation energy can be directly calculated from the differential data, which can accurately distinguish the pyrolysis behaviour of different stages. For the oil shales of the Xiamaling Formation, Brazilian Irati, Chang 7 and Qing 1 Members, the FWO and KAS methods can be used. Their activation energy changes with the conversion rate, and the model-free isoconversional methods can reflect the dynamic change in activation energy without presetting a model. The FWO and KAS methods have higher accuracy at high conversion rates and are suitable for marine oil shales or samples containing complex minerals.

**Table 1.** Classification of Kinetic Methods.

| Kinetic Method | Typical Oil Shale | Reaction Model | Activation Energy Range |
|---|---|---|---|
| Coats–Redfern | Huadian, Maoming, Fushun Oil Shales | Single Reaction Model | 80–150 kJ/mol |
| Arrhenius | Huadian, Fushun Oil Shales | Single Reaction Model | 80–150 kJ/mol |
| Friedman | Longkou, Green River, Liushuhe Oil Shales | Multi-stage Reaction Model | 100–200 kJ/mol |
| FWO, KAS | Xiamaling Formation, Brazilian Irati, Chang 7 Member, Qing 1 Member | Conversion-dependent Model 150–300 kJ/mol | 150–300 kJ/mol |

## 3. In Situ Pyrolysis Technology Methods of Oil Shale

### *3.1. Current Status of Oil Shale Above-Ground Retorting Technology*

Surface retorting technologies work primarily by mining oil shale to the ground surface, where heat is supplied to oil shale particles via gaseous or solid heat carriers within controlled reactors to induce thermal cracking of kerogen. A key advantage is that temperature, heating rate, residence time and product discharge conditions can be readily regulated. For this reason, surface retorting has long served as an important experimental foundation for investigating pyrolysis mechanisms and hydrocarbon yields of oil shale.

Available surface retorting technologies are mainly categorized into gaseous heat carrier and solid heat carrier types. Variations among different processes lie primarily in heat supply modes, particle sizes, heat transfer pathways and product residence time. Since surface retorting generally employs crushed oil shale particles, its heat transfer distance is substantially shorter than that in subsurface reservoirs. Consequently, pyrolysis temperatures can be achieved within a short period, yet the conditions for hydrocarbon generation and migration are altered simultaneously.

Therefore, the main value of surface retorting studies does not lie in directly representing in situ pyrolysis processes. Instead, it delivers fundamental understandings for in situ pyrolysis in three respects: first, identifying the basic temperature window and reaction stages of kerogen pyrolysis; second, acquiring kinetic parameters and generation patterns of oil, gas, coke and other products; third, revealing how factors such as heating rate, particle size, pressure and residence time affect product distribution. Meanwhile, remarkable discrepancies exist between surface retorting and subsurface reservoirs in terms of heat transfer scale, pressure, fluid transport and pore structure. Hence, experimental results cannot be directly extrapolated to in situ pyrolysis without correction. In situ conversion studies demonstrate that subsurface pyrolysis requires concurrent consideration of heat transfer, product migration and pyrolysis-induced pore fracture evolution.

The Table 2 summarizes advanced surface retorting processes worldwide, outlining their forms, retorting schemes, oil recovery rates and technical characteristics.

Despite decades of industrial application and mature surface retorting equipment, comprehensive progress reviews continuously highlight that above-ground oil shale retorting suffers from critical drawbacks [40,41]. These include limited resource efficiency for fine particles, significant thermal heat loss and severe environmental pollution (e.g., spent shale, dust and VOCs). Moreover, researchers analyzing low-temperature pyrolysis processes on the surface note persistent challenges in energy structure optimization and emission controls, which conflict with modern clean production strategies [42,43].

1. Particle Size Limitation and Resource Waste

Most above-ground retorts impose strict particle size requirements. For example, Kiviter and Fushun retorts are only suitable for lump oil shale (25–100 mm), while Galoter and ATP can process finer particles (<25 mm) but still cannot effectively utilize particles below 3 mm. Consequently, a considerable amount of fine shale is discarded or inefficiently used, leading to resource waste.

2. Unfavourable Thermal Efficiency and Energy Structure

Although solid heat carrier processes (e.g., Lurgi-Ruhrgas, Galoter) exhibit relatively high thermal efficiency, they suffer from complex equipment, coking and clogging issues. Gaseous heat carrier processes (e.g., Fushun retort) are simpler in structure but generally have lower thermal efficiency, with substantial heat loss through exhaust gases and high energy consumption for carrier gas circulation.

3. Limited Pollution Control Capacity

Above-ground retorting generates significant amounts of spent shale, dust, sulfur-containing wastewater and volatile organic compounds (VOCs). Traditional retorts, such as the Fushun and Kiviter types, are often equipped with rudimentary off-gas treatment systems, making it difficult to meet stringent emission standards. This conflicts with the "dual carbon" strategy that demands cleaner production.

4. Discrepancy Between Oil Yield and Laboratory Results

The high oil yields listed in Table 2 (e.g., Tosco-II 100%, Galoter > 90%) are typically obtained under short-term, optimized conditions. In long-term industrial operation, factors

such as uneven particle mixing, temperature fluctuations and variations in oil shale grade often reduce the actual yield to only 60–80% of the laboratory value.

**Table 2.** Above-ground Retorting Technologies.

| Retort Name | | Country of Origin | Type | Heat Carrier | Daily Processing Capacity (t/d) | Particle Size | Retorting Process | Oil Yield (%) | Technical Characteristics |
|---|---|---|---|---|---|---|---|---|---|
| Solid Heat Carrier | Lurgi-Ruhrgas | Germany | Twin-Screw Spiral | Shale Ash | 1600 | <5 | Oil Shale Pyrolysis, Residue Combustion | >90 | High oil yield and low energy consumption, but discharge system prone to clogging |
| | Tosco-II | USA | Inclined Rotary Drum | Ceramic Balls | 1000 | <12.7 | Oil Shale Pyrolysis, Residue Cooling | 100 | High oil yield, but complex equipment structure |
| | Galoter | Estonia | Cylindrical Rotary | Shale Ash | 3000 | <25 | Oil Shale Pyrolysis, Residue Combustion | >90 | Simple structure and low investment, but can only process lump samples |
| | ATP Retort | Canada | Cylindrical Rotary | Shale Ash | 6000 | <25 | Oil Shale Pyrolysis, Residue Combustion | >90 | Self-sufficient in energy and high utilization rate, but complex structure |
| Gaseous Heat Carrier | SGR | USA | Vertical Conical | Retort Gas | 10,000 | 3.2~50.8 | Oil Shale Pyrolysis, Residue Gasification | 85~100 | High oil yield and low energy consumption, but discharge system prone to clogging |
| | Petrosix | Brazil | Vertical Cylinder | Retort Gas | 6240 | 8~50 | Oil Shale Pyrolysis, Residue Cooling | >90 | Strong daily processing capacity, but can only process lump samples |
| | Kiviter | Estonia | Vertical Cylinder | Retort Gas | 1000 | 25~100 | Oil Shale Pyrolysis, Residue Cooling | 75~80 | Simple structure and low investment, but can only process lump oil shale |
| | Fushun | China | Vertical Cylinder | Retort Gas | 100 | 10~75 | Oil Shale Pyrolysis, Residue Gasification | 65 | Simple structure and mature technology, but low heating efficiency |

### *3.2. Current Status of Oil Shale In Situ Conversion Technology*

Unlike surface retorting, in situ oil shale pyrolysis does not require mining the entire reservoir to the surface. Instead, kerogen undergoes thermal cracking within the reservoir through subsurface heating, and the generated hydrocarbons are delivered to production wells via naturally occurring or artificially created pore fracture channels. Consequently, the core challenge of in situ pyrolysis shifts from "how to heat particles rapidly" to "how to achieve effective heat supply, reaction and product transport at the subsurface reservoir scale".

According to the dominant heat transfer mode, existing in situ pyrolysis technologies can be categorized into four types: conduction heating, convection heating, reaction-heat heating and radiation heating. Recent review studies generally adopt this classification Figure 2. Shell ICP and ExxonMobil Electrofrac are typically assigned to conduction heating; Chevron CRUSH and MTI to convection heating; self-heating or chemical-reaction-based heat supply methods to reaction-heat heating; and radio-frequency and microwave methods to radiation heating.

For in situ conversion, heat is introduced directly into underground formations. (**1**) **Conductive heating**, best represented by the in situ conversion process (ICP), has demonstrated relatively high engineering maturity. Extensive pilot tests, sometimes combined with water vapour injection for upgrading, have proven its feasibility [7,44]. To optimize this slow heating process, recent engineering efforts have focused heavily on large-scale numerical simulation for vertical and horizontal well pattern designs [45,46]. (**2**) **Convective heating** accelerates heat transfer by injecting high-temperature fluids. Advanced methodologies utilizing steam injection [47] or supercritical $CO_2$ [48] are actively investigated, though engineers must carefully control fluid mobility and the migration of

pollutants along high-permeability channels [49]. (**3**) **Radiative heating**, such as electric, microwave or RF heating, provides localized volumetric heating, significantly impacting hydrocarbon generation and accelerating pore evolution in tight basins like North Songliao [50]. (**4**) **Reactive/Autogenous heating**, which relies on topochemical or in situ chemical reactions (e.g., autogenous thermal transformation), has emerged as a highly efficient alternative to drastically reduce external energy consumption while maintaining optimal production [51–53].

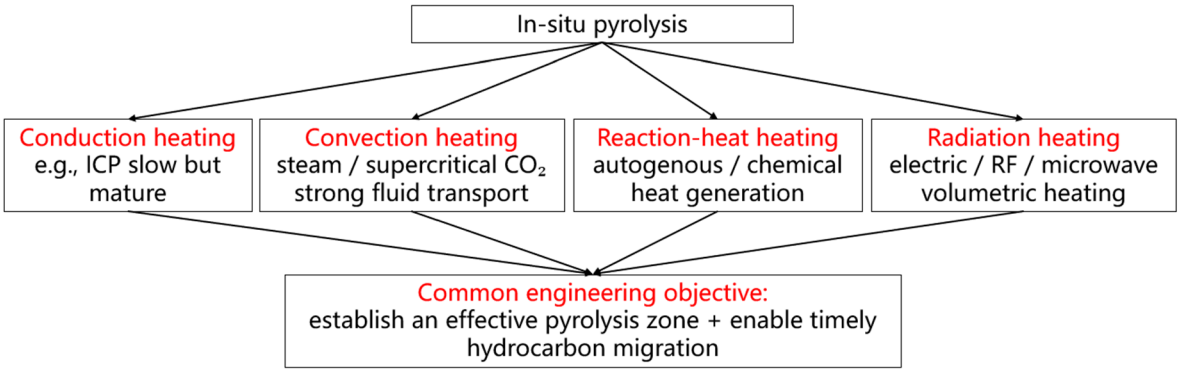


**Figure 2.** Classification of in situ oil shale pyrolysis technologies by dominant heat transfer mode.

On the whole, no absolute superiority exists among different in situ pyrolysis technologies; rather, they correspond to different reservoir conditions and engineering objectives. Conduction heating offers high technical maturity but slow heating rates. Convection heating strengthens heat transport but depends strongly on fractures and permeability. Reaction-heat heating holds potential for reducing external energy demand, yet involves complex reaction processes. Radiation heating enables rapid volumetric heating, but equipment and energy concerns persist. More importantly, all in situ pyrolysis technologies must ultimately resolve the same fundamental issue: establishing a sufficiently large effective pyrolysis zone within the reservoir, and ensuring that generated hydrocarbons can be transported in time to production wells through continuously evolving pore fracture networks. Therefore, in situ pyrolysis research should shift from mere "comparison of heating methods" toward integrated analysis of "heat transfer–reaction–seepage–reservoir structural evolution".

## 4. Research on In Situ Pyrolysis Kinetic Models and Methods

At present, kinetic modelling is universally recognized as the most critical theoretical basis for simulating oil shale pyrolysis [1,54]. Early foundational studies on particle pyrolysis kinetics established the basic framework for predicting thermal decomposition [4,6]. The most common approach utilizes thermogravimetric analysis (TGA).

### *4.1. Arrhenius Plotting Method*

The Arrhenius plot is a traditional experimental method for calculating the activation energy ($E_a$) and pre-exponential factor (A). Its core idea is to convert the Arrhenius equation into a linear relationship. Based on the Arrhenius equation:

$$k = A\exp\left(-\frac{E_a}{RT}\right) \quad (1)$$

where k is the reaction rate constant, A is the pre-exponential factor, $E_a$ is the activation energy, R is the gas constant, and T is the absolute temperature. Taking the natural logarithm on both sides of the equation, a linear form is obtained:

$$lnk = -\frac{E_a}{RT} \cdot \frac{1}{T} + lnA \quad (2)$$

by plotting a straight line of lnk versus $\frac{1}{T}$, the activation energy can be calculated from the slope, and the pre-exponential factor can be calculated from the intercept.

Lv Xiaoshu et al. proposed an improved model that does not make any assumptions about temperature integration or kinetic mechanisms, effectively making up for the limitations of the Arrhenius method. The model developed using the constant heating rate:

$$\beta = \frac{dT}{dt} \quad (3)$$

provides a closed-form expression for decomposition kinetics based on kinetic parameters, which is simple, efficient and fully automated. However, the accuracy of the improved reaction model depends on the temperature interval ΔT, so a large temperature increment (at least 25 °C) is required for accurate results. Li Shuyuan and Yue Changtao established a kinetic model consisting of 11 parallel reactions based on the Arrhenius method. For each parallel reaction, the final conversion rate and apparent frequency factor were calculated from the weight loss data, and the correlation equations of $x_\infty$ (conversion rate) -E and $lnA - E$ were obtained. The final conversion rate can be expressed as an exponential function of the corresponding activation energy. Pankaj Tiwari and Milind Deo used a model-free conversion method based on the Arrhenius equation, and the calculated activation energy was a function of the conversion rate, with a maximum uncertainty of approximately 10% of the calculated energy value. This model method is more intuitive and fast for parameter fitting using power laws, activation energy distributions and discrete energy values within a specific conversion interval, but it has poor adaptability in reproducing multi-step kinetics.

The Arrhenius plot remains a foundational tool. Researchers have extensively utilized non-isothermal kinetic experiments based on the Arrhenius equation to optimize processing conditions [14]. By integrating TGA and TGA-MS data, detailed compositional and kinetic analyses by Tiwari et al. demonstrated that calculated activation energy often functions dependently on the conversion rate [12,13]. Similarly, Kök and Pamir determined pyrolysis kinetics using DSC and TG/DTG, identifying linear regions mapped directly to the Arrhenius model [55]. To overcome the limitations of preset temperature integrations, Lü X. S. et al. proposed a generalized and efficient analytical approach that operates independently of kinetic mechanism assumptions [56]. For shales exhibiting complex heterogeneous reactions, Li S. Y. and Yue C. T. formulated an advanced model comprising 11 parallel Arrhenius reactions [57,58], which was subsequently adapted to characterize pyrolysis kinetics in the presence of water [59].

### *4.2. Coats–Redfern Method*

The Coats–Redfern method provides a robust integral approximation. It has been effectively employed by Wang Z. J. et al. to study the kinetics of Huadian oil shale, spent shale and their mixtures [60]. Furthermore, Jiang H. et al. applied this method to quantitatively assess how varying pyrolysis conditions and the addition of transition metal salts influence product yields [34]. In analyzing Beizao oil shale, Zhang J. et al. simplified and improved the original first-order Coats–Redfern equation, establishing regression equations to clarify multi-stage reaction mechanisms [61].

The Coats–Redfern method is a classic integral method for calculating the kinetic parameters of solid pyrolysis based on thermogravimetric analysis (TGA) data. Proposed by Coats and Redfern in 1964, it is widely used in the kinetic analysis of pyrolysis of complex solid materials such as oil shale, coal and biomass. Through the integral approximation of the Arrhenius equation, the non-linear relationship is converted into a linear form. For a first-order reaction (n = 1), the Coats–Redfern equation is obtained:

$$\ln\left[\frac{-\ln(1-x)}{T^2}\right] = \ln\left(\frac{AR}{\beta E}\cdot\frac{1-2RT}{E}\right) - \frac{E}{RT} \tag{4}$$

where x is the conversion rate, R is the gas constant, T is the absolute temperature, A is the pre-exponential factor, E is the activation energy, and β is the constant heating rate.

Jiang Haifeng et al. [34] calculated the pyrolysis kinetic parameters with and without catalysts using the Coats–Redfern method. The apparent activation energy and pre-exponential factor were determined according to the slope and intercept in the plot of

$$\ln\left[\frac{-\ln(1-x)}{T^2}\right] \text{ versus } \frac{1}{T}. \tag{5}$$

The results showed that the use of transition metal salts reduced the apparent activation energy in the main pyrolysis stage. Paul T. Williams et al. [14] simplified the Coats–Redfern equation and plotted the relationship between

$$\ln\left[\frac{-\ln(1-x)}{T^2}\right] \text{ and } \frac{1}{T}. \tag{6}$$

The decomposition of oil shale was regarded as a single-step process at a heating rate of 5 k/min to determine its reaction order. Compared with the activation energy obtained by the Arrhenius method, the calculated activation energy was smaller, and the results showed that the heating rate had no significant effect on the activation energy. Juliana Pedrilho Foltin et al. used the Coats–Redfern method, introduced the mass of oil shale before and after pyrolysis ($m_0$, $m_f$), and calculated the pyrolysis kinetic parameters from the thermogravimetric analysis data. The results showed that the parameters measured by this method were insensitive to the heating rate, and the obtained activation energy was low, which did not conform to the actual situation. M.V. KÖK and R. PAMIR used the Coats–Redfern model method, assumed the reaction order n, obtained a straight line with a slope of $-\frac{E}{R}$ by calculating and experimentally fitting the correct n value and determined the activation energy accordingly. Zhang Juan, Ding Yanming et al. [61] simplified and improved the original first-order Coats–Redfern equation under the condition of constant heating rate and established a regression equation between $\ln\left(\frac{g(\alpha)}{T^2}\right)$ and $\frac{1}{T}$ to determine the kinetic parameters. The results further confirmed that the pyrolysis kinetic process has multiple stages, and

$$g(\alpha) = [-\ln(1-\alpha)]^2 \tag{7}$$

was determined as the best mechanism for describing the first stage, and

$$g(\alpha) = [-\ln(1-\alpha)]^3 \tag{8}$$

was used for the second stage.

### *4.3. Friedman Method*

The Friedman method is a classic model-free differential method proposed by Howard L. Friedman in 1964. It is mainly used to extract reaction kinetic parameters from TGA

data and is suitable for multi-step reaction processes such as pyrolysis and degradation of complex solid materials (such as oil shale, coal and biomass). Its core advantage is that it does not require presetting a reaction model and can directly calculate kinetic parameters from experimental data, avoiding errors caused by improper model assumptions. Based on the basic kinetic equation of solid reactions and the Arrhenius equation, the Friedman equation is derived:

$$\ln\left(\frac{d\alpha}{dt}\right) = \ln(A \cdot f(\alpha)) - \frac{E}{RT} \tag{9}$$

for the same conversion rate $\alpha$, f($\alpha$) is a constant.

Juliana Pedrilho Foltin used the Friedman equation and introduced the mass of oil shale before and after pyrolysis ($m_0, m_f$) to solve the kinetic parameters. This method is sensitive to the transition process (conversion rate) from the thermal cracking zone to the mineral-assisted cracking zone. At low conversion rates, when the total reaction rate is high and the signal-to-noise ratio of the data is also high, the accuracy of this method is high. Li Shuyuan and Yue Changtao used a special regression function to calculate the pyrolysis reaction rate and applied the Friedman equation to obtain kinetic parameters [32]. A series of different conversion rate values were selected as constants, and the activation energy and frequency factor at each conversion rate were determined by linear regression of $\ln(\frac{\mathrm{dx}}{\mathrm{dt}})$ versus $\frac{1}{T}$.

### *4.4. FWO Method and KAS Method*

Both Flynn–Wall–Ozawa (FWO) and Kissinger–Akahira–Sunose (KAS) are model-free kinetic analysis methods based on thermogravimetric analysis (TGA) data. The former was independently proposed and improved by Flynn, Wall and Ozawa, while the latter was successively proposed and improved by Kissinger, Akahira and Sunose. They are widely used in the calculation of kinetic parameters for complex reactions such as pyrolysis and degradation of solid materials (such as oil shale, coal and biomass). Their core advantage is that they do not require presetting a reaction model and can directly solve the activation energy through experimental data at different heating rates, avoiding errors caused by improper model assumptions. Based on the kinetic equation of solid reactions and the Arrhenius equation, the FWO equation is derived:

$$\ln(\beta) = \ln\left(\frac{\mathrm{AE}}{\mathrm{Rg}(\alpha)}\right) - 5.331 - 1.052\frac{E}{RT} \tag{10}$$

and the KAS equation is:

$$\ln\left(\frac{\beta}{T^2}\right) = \ln\left(\frac{AR}{Eg(\alpha)}\right) - \frac{E}{RT} \tag{11}$$

where g($\alpha$) is the integral form of the reaction model function f($\alpha$).

Cao Ran, Yang Dong et al. [33] used the FWO and KAS methods to determine the kinetic parameters. For the former, when the conversion rate is constant, linear fitting of $\ln(\beta)$ and $\frac{1}{T}$ gives a straight line, and the apparent activation energy is obtained according to the slope of the straight line, which is 1.052 $\frac{E}{R}$. Among them, the integral mechanism function

$$\mathrm{g}(\alpha) = \frac{AE}{\beta R}P(u), P(u) = 0.00484 \cdot \exp(-1.015 - 6\mathrm{u}) \tag{12}$$

represents the temperature integral. For the KAS method, after linear fitting of $\ln\left(\frac{\beta}{T^2}\right)$ and $\frac{1}{T}$, the slope of the straight line is $\frac{E}{R}$, and the approximate value of the apparent activation energy is calculated accordingly. Zhao Shuai et al. used the Doyle temperature integral formula based on the FWO equation [62]. By plotting $\ln(\beta)$ versus $-\frac{1}{T}$, under different

conversion rate conditions, the slope obtained by fitting the curve with a first-order function is k = 0.4576 $\frac{E}{R}$. The results showed that the calculated activation energy increases with the increase in conversion rate. Through the KAS method, the mass of oil shale pyrolysis was introduced to express the conversion rate:

$$\alpha = \frac{m_0 - m}{m_0 - m_\infty} \tag{13}$$

and the plot of ln(β) versus $-\frac{1}{T}$ under different conversion rates was drawn. The slope obtained by fitting the curve with a first-order function is k = $\frac{E}{R}$. Ely Cheikh Moine et al. [10] rearranged and combined the Arrhenius equation, derived the possible mechanism function:

$$g(\alpha) = \frac{AEe^{-x}}{\beta RX^2} h(x) \tag{14}$$

and substituted it into the FWO equation to solve the apparent activation energy. Juliana Pedrilho Foltin et al. used the FWO method to calculate the pyrolysis kinetic parameters, where

$$f(\alpha) = (1 - \alpha)^n \tag{15}$$

Under the condition of high conversion rate (when the reaction rate is low), the kinetic parameters calculated by this method are more accurate.

### *4.5. Extension of Kinetic Parameters to Hydrocarbon Generation Prediction*

Traditional kinetic studies on oil shale pyrolysis typically focus on the estimation of activation energy and pre-exponential factor. For in situ pyrolysis research, however, obtaining kinetic parameters alone cannot directly resolve the issue of oil gas production prediction. The genuine engineering value of kinetic parameters lies in converting the temperature field into kerogen conversion and further establishing material transformation relationships from kerogen to liquid hydrocarbons, gaseous hydrocarbons and solid residues.

When product generation is additionally considered, serial or parallel reaction models can be adopted. For example, studies on Kukersite oil shale employ a serial first-order reaction model of "kerogen → pyrobitumen → shale oil + gas", with kinetic parameters for both reaction stages derived experimentally. The results reveal that kerogen is first converted predominantly into pyrobitumen, which subsequently decomposes into shale oil and gas. This suggests that a single-step "kerogen → oil + gas" model may not adequately describe the actual pyrolysis process.

For Green River oil shale, the generalized kinetic model developed by Burnham and Braun further accounts for the generation of oil, water and gas from kerogen, as well as oil coking and cracking. This demonstrates that oil shale pyrolysis models can evolve from single kerogen conversion into multi-component, multi-reaction pathway frameworks.

Consequently, in numerical simulation of in situ pyrolysis, kinetic models must accomplish at least three hierarchical conversions: first, calculating kerogen reaction rates based on local temperature; second, deriving kerogen conversion and intermediate-product generation from these rates; and third, determining the yields of liquid hydrocarbons, gaseous hydrocarbons and coke according to different reaction pathways. Existing in situ numerical simulations have already coupled chemical kinetics, heat conduction, phase equilibrium and mass transport to predict hydrocarbon generation and migration under subsurface heating conditions.

Therefore, the significance of model-free kinetic methods such as Friedman, FWO and KAS extends beyond yielding a set of activation energies; it lies in providing conversion-

dependent kinetic parameters for subsequent reaction rate models. When activation energy varies significantly with conversion, piecewise or continuous functions can be used to describe E(α), which is then embedded into the reaction source term, thereby describing the multi-stage pyrolysis process of oil shale more reasonably. Studies on Irati oil shale show that, within a conversion range of 0.15–0.55, activation energy increases from approximately 215 kJ/mol to 255 kJ/mol, indicating that describing the entire pyrolysis process with a fixed activation energy may mask pronounced differences among reaction stages.

It is thus evident that oil shale pyrolysis kinetics research should evolve from "calculating kinetic parameters" toward "utilizing kinetic parameters to predict conversion and products". This shift is especially critical for in situ pyrolysis, because subsurface reservoirs feature pronounced spatial temperature gradients; the ultimate oil gas generation volume depends on the temperature–time history experienced at different locations, rather than a single final temperature.

## 5. Pyrolysis Process and Hydrocarbon Generation of Oil Shale

### *5.1. Stage-Dependent Characteristics of Oil Shale Pyrolysis*

Oil shale pyrolysis is a complex process involving continuous transformation of diverse organic structures, accompanied by volatile release, secondary cracking and mineral reactions. As the primary hydrocarbon-generating organic matter in oil shale, kerogen cannot be directly converted into final liquid oil and gaseous hydrocarbons in a single step upon heating. Existing thermal analysis and retorting experiments demonstrate that oil shale pyrolysis can generally be divided into several stages with distinct reaction features according to variations in mass loss, reaction rate and product composition. Extensive mechanistic reviews and comprehensive kinetics studies demonstrate that oil shale pyrolysis can be mechanistically generalized into three stages: low-temperature volatile release, major kerogen pyrolysis and high-temperature secondary cracking coupled with mineral reactions [20,35].

Existing thermal analysis and retorting experiments demonstrate that oil shale pyrolysis can generally be divided into several stages with distinct reaction features according to variations in mass loss, reaction rate and product composition. Although discrepancies exist in the temperature ranges for stage division among different studies owing to variations in oil shale type, kerogen composition, mineral content, experimental atmosphere, heating rate and sample particle size, oil shale pyrolysis can be mechanistically generalized into three stages: low-temperature volatile release, major kerogen pyrolysis and high-temperature secondary cracking coupled with mineral reactions.

In the low-temperature stage, mass variation of samples is mainly associated with the escape of pore water, adsorbed water and a small amount of low-molecular-weight volatile components, while massive cracking of the kerogen matrix does not occur. Hence, this stage is normally characterized by slight mass loss and low reaction rate. For oil shale with high water content or well-developed pore structures, more remarkable mass variation can be observed in the low-temperature stage; nevertheless, such mass change is not predominantly contributed by hydrocarbon generation.

As the temperature further rises, weak bonds and thermally labile organic moieties within kerogen start to break, marking the onset of the major pyrolysis stage. The reaction rate increases sharply at this stage, generating abundant organic intermediates and volatile products. This corresponds to the principal temperature window for the formation of liquid and gaseous hydrocarbons. The onset and peak temperatures of this stage vary for different oil shale samples. Kerogen enriched in reactive organic structures generally exhibits a lower initial pyrolysis temperature, whereas organic matter with high thermal stability requires higher temperatures to achieve considerable conversion.

With continuous temperature elevation, the primary conversion of pristine kerogen is gradually accomplished. Nevertheless, heavy intermediates formed in the preceding process may further undergo cracking and polycondensation reactions. Part of heavy liquid products are further cracked into light oil and gaseous hydrocarbons, while others may form coke via polycondensation. Consequently, the product composition in the high-temperature stage differs substantially from that in the major pyrolysis stage. In addition, for oil shale containing abundant carbonate minerals, carbonate decomposition may take place with $CO_2$ release in the high-temperature stage, giving rise to extra mass loss.

### *5.2. Primary Pyrolysis and Conversion Process of Kerogen*

Kerogen is the dominant hydrocarbon-generating organic matter in oil shale, whose structure consists of various aliphatic chains, aromatic moieties, heteroatom-containing functional groups and chemical bonds. At the initial pyrolysis stage, thermally labile organic structures break preferentially to yield intermediate organic products with high molecular weights. Mechanistic studies tracking this primary conversion confirm that these intermediates predominantly manifest as thermal bitumen [1,21]. As temperature increases, these intermediate products undergo further cracking and gradually produce liquid and gaseous hydrocarbons. Moreover, research conducted under semi-open conditions highlights that the overall kerogen conversion involves complex, multi-pathway generation of oil, water and gas, meaning intermediate products continuously evolve as the reaction progresses [18].

Accordingly, the reaction pathway of kerogen pyrolysis can be simplified as Figure 3:

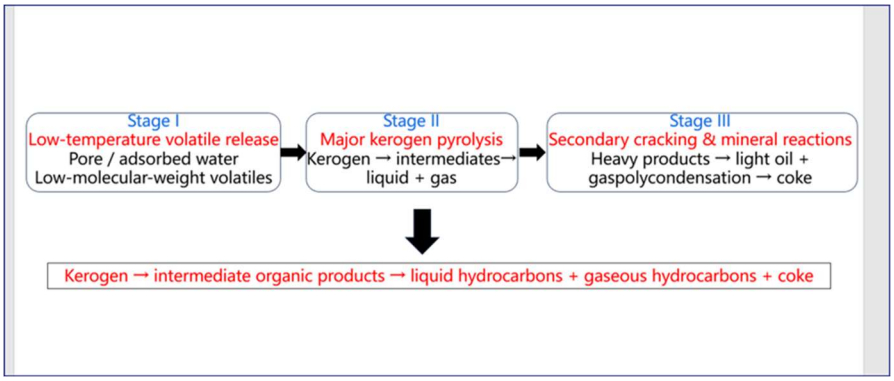


**Figure 3.** Schematic reaction pathway and stage-dependent product evolution during oil shale pyrolysis.

Kerogen → Intermediate organic products → Liquid hydrocarbons + Gaseous hydrocarbons + Coke.

Herein, intermediate organic products refer to asphaltenes, heavy organics and other volatile intermediates generated during the primary cracking of kerogen. This process presents obvious conversion-dependent behaviours. At low conversion levels, thermally vulnerable organic structures react preferentially, which may lead to low apparent activation energy. As the reaction proceeds, the residual organic matter becomes progressively more thermostable, and higher energy is required for further cracking, resulting in the variation in activation energy with conversion degree. This accounts for why isoconversional kinetic methods including FWO and KAS can reflect the complexity of oil shale pyrolysis.

After kerogen conversion, carbon and hydrogen elements can partition into liquid hydrocarbons, gaseous hydrocarbons, coke and other products. Therefore, even at identical kerogen conversion ratios, diverse hydrocarbon product ratios can still be obtained under different temperatures, pressures, residence times and mass transfer conditions. For instance, considerable heavy intermediates are generated from primary kerogen cracking

at relatively low pyrolysis temperatures, and part of such intermediates can be further converted into liquid oil. When the temperature rises continuously, heavy products may be further cracked into light gaseous hydrocarbons. Consequently, to evaluate whether a given pyrolysis condition is favourable for oil production, it is insufficient to merely compare kerogen conversion extent; the evolution of liquid and gaseous products should also be analyzed simultaneously.

### 5.3. Effects of Secondary Cracking on Hydrocarbon Composition

Secondary cracking represents a critical process governing product composition during high-temperature pyrolysis. Secondary cracking refers to the continuous chemical bond cleavage of liquid or heavy organic products already formed by primary kerogen pyrolysis under higher-temperature or longer-residence-time conditions. Advanced numerical simulations targeting the hydrocarbon generation process during in situ conversion reveal that this process falls into two main consequences [9,17]: on the one hand, heavy organic substances crack into light liquid and gaseous hydrocarbons, lowering the average molecular weight of oil products; on the other hand, partial organic intermediates may undergo polycondensation and aromatization, ultimately forming solid residues such as coke. Therefore, controlling secondary cracking is fundamental to maximizing the liquid-oil yield.

Higher pyrolysis temperature does not always favour resource utilization. If the research objective is to maximize liquid-oil yield, sufficient kerogen conversion should be ensured while the residence time of liquid products in high-temperature zones should be minimized. For surface retorting, secondary cracking can be mitigated by regulating heating rate, particle size and product discharge rate. For in situ pyrolysis, the extent of high-temperature zones and the residence time of generated products need to be controlled by adjusting reservoir temperature distribution, heating duration, fluid flow velocity and production-well pressure.

## 6. Factors Influencing Oil Shale Pyrolysis

Oil shale pyrolysis is a process jointly affected by heat transfer, mass transfer and chemical reactions, involving various chemical reactions and physical changes, and hundreds of intermediate chemical products. It is affected by the physicochemical properties of oil shale, such as the particle size, chemical composition and mineral content of oil shale, as well as the pyrolysis process conditions, such as retorting temperature, residence time, heating rate, retorting medium and reactor structure. Comprehensive analyses of the factors affecting oil shale pyrolysis emphasize that by investigating the influence of different reaction conditions on the yield distribution and oil/gas characteristics, the pyrolysis process can be optimized to maximize the energy utilization rate [42].

### 6.1. Material Properties (Particle Size)

The composition and particle size of oil shale are its material properties. Firstly, the main component of oil shale is minerals, accounting for 65–80% of the total minerals, mainly including carbonates, silicates, etc. Most oil shales can not only decompose under heating conditions but also react with certain substances, thereby affecting the pyrolysis process and product yield. Compared with other components, silicates have a significant inhibitory effect on the thermal cracking of oil shale.

In the pyrolysis reaction, oil shale with different particle sizes will affect its heating rate and volatile release rate, thereby affecting the entire pyrolysis process. Zhang Jianjian et al. conducted thermogravimetric analysis on oil shale with different particle sizes under the same temperature conditions, showing that when the particle size is larger than 1–3 mm, the thermal weight loss reaches its maximum, confirming that particle size is a primary

factor affecting heat transfer [63]. Furthermore, the research of Khalil et al. showed that the oil absorption rate of oil shale first increases and then decreases with the increase in particle size; especially after 10–20 mm, the oil solubility increases, thereby accelerating oil shale pyrolysis [3]. Increasing the shale particle size within an appropriate range can effectively increase the oil recovery rate.

### 6.2. Heating Rate

With the increase in heating rate, the initial pyrolysis temperature, peak temperature and final temperature all show a linear relationship. Zhao S, Sun Y et al. studied different heating rates during the pyrolysis of oil shale and found that with the continuous increase in heating rate, the main pyrolysis region moves to a higher-temperature region [62]. Similarly, the research of Bai F et al. found that with the increase in heating rate, the main stage of oil shale pyrolysis moves to a higher-temperature range, and the initial and final pyrolysis temperatures also increase accordingly [11]. However, Al-Ayed O S et al. found in experiments that increasing the heating rate of oil shale can sometimes reduce the final oil recovery rate, an effect closely related to secondary cracking and the demineralization state of the samples [64,65].

### 6.3. Pyrolysis Temperature

The influence of pyrolysis temperature on the oil shale pyrolysis process is relatively complex, mainly manifested in the change in the final pyrolysis temperature, oil yield, composition, generation of pyrolysis semicoke and the occurrence of secondary pyrolysis. Studies by Wang S., Jiang X. M. et al. exploring the mechanism and kinetics observed that increasing the pyrolysis temperature leads to an increase in the N content in shale oil, while the H/C ratio and O content decrease, indicating that pyrolysis temperature deeply affects the elemental composition of shale oil [1,66]. Additionally, applying different thermal treatment temperatures fundamentally influences the pore evolution of the matrix, which indirectly controls how efficiently products can escape from the high-temperature zone [38].

### 6.4. Pressure

The effect of pressure on oil shale pyrolysis is not necessarily unidirectional and depends on the pressure range, reaction environment, oil shale composition, and whether the measured response is an onset temperature, volatilization behaviour, oil yield or product composition. Pressurized TGA studies have reported that increasing pressure can shift hydrocarbon volatilization to higher temperatures and reduce oil yield, whereas other studies report a decrease in the initial pyrolysis temperature with increasing pressure [19,25]. These apparently different observations should therefore be interpreted in the context of the specific experimental conditions rather than treated as a universal pressure effect. Under in situ conditions, pressure also changes phase equilibrium and product transport, thereby affecting secondary cracking and final hydrocarbon composition [67].

### 6.5. Coupled Heat Transfer, Mass Transfer, Reaction Effects and Their Absence in TGA Studies

In real in situ pyrolysis, the situation is drastically different from TGA experiments: heat conduction in large-scale rock masses is slow, volatile migration is hindered in the tight shale matrix, and fracture opening/closing under geostress dynamically alters heat and mass transfer pathways. Consequently, researchers have observed a continuous evolution of anisotropic thermophysical, hydraulic and mechanical characteristics during the heating process [68,69]. Furthermore, the strong temperature dependence of pore structure significantly governs the dynamic variation in reservoir porosity and permeability [15,16]. Therefore, directly extrapolating in situ pyrolysis behaviour from TGA

parameters carries serious risks. To realize the transition from "kinetic parameter computation" to "reservoir-scale hydrocarbon production prediction", future studies must develop large-scale multi-field coupled numerical models and physical simulation tests capable of accurately capturing the complex in situ thermo-hydro-mechanical–chemical (THMC) conditions [70–74].

## 7. Conclusions

(1) Pyrolysis behaviours of oil shales from different regions exhibit distinct petrological and organic–geochemical discrepancies. Kerogen type, thermal maturity, organic matter abundance and mineral composition jointly determine the initial pyrolysis reactivity and inherent hydrocarbon generation potential of oil shale. Accordingly, kinetic parameters and product yields of oil shales from various regions cannot be simply described by uniform values. Typical oil shale deposits including Green River, Fushun, Maoming, Estonian Kukersite and Brazilian Irati are selected in this work to cover diverse kerogen architectures, mineral assemblages and experimental conditions, rather than to represent all oil shale occurrences worldwide.

(2) Oil shale pyrolysis is not a single kerogen-cracking event but a multi-stage process involving kerogen structural rearrangement, pyrobitumen formation, liquid- and gaseous-hydrocarbon generation, secondary cracking, coking and mineral-mediated reactions. Experimental observations demonstrate that kerogen first yields intermediate products such as pyrobitumen, which are further converted into liquid and gaseous hydrocarbons. With continuous increases in temperature and residence time, portions of heavy-weight products undergo further cracking or polycondensation. Hence, the influence of pyrolysis temperature on hydrocarbon yields does not follow a simple monotonic relationship.

(3) Mineral composition and pore structure serve as critical links bridging pyrolysis reactions and reservoir seepage. Minerals modify rock thermophysical properties and organic matter occurrence modes and may also affect adsorption–desorption behaviours and secondary reactions of pyrolysis products. Meanwhile, newly generated pores and fractures originating from kerogen pyrolysis improve product transport capacity and trigger dynamic evolution of reservoir permeability. Consequently, prominent feedback coupling exists among "pyrolysis reaction–pore evolution–fluid transport" during in situ pyrolysis.

(4) Research priorities for kinetic models should shift from pure activation energy calculation toward hydrocarbon generation prediction. The Arrhenius and Coats–Redfern approaches are suitable for constructing kinetic models with explicit reaction assumptions. By contrast, isoconversional methods including Friedman, FWO and KAS can obtain apparent activation energies varying with conversion degree and are better suited for characterizing the multi-stage and heterogeneous nature of oil shale pyrolysis. Existing studies have further incorporated kinetic parameters into serial or parallel reaction models, achieving quantitative description covering kerogen conversion and the formation of pyrobitumen, oil, gas and coke.

(5) Particle size, heating rate, pyrolysis temperature, pressure and residence time exert strongly coupled effects on pyrolysis products. Particle size influences pyrolysis mainly via heat transfer and volatile-species diffusion. There generally exists an optimal heating rate window favouring primary pyrolysis while suppressing secondary cracking. Elevated temperature accelerates kerogen conversion, yet excessive temperature may intensify secondary cracking and coking. Pressure modulates final product distribution through product escape, phase equilibrium and mass transfer processes. Isolated analysis of a single factor tends to yield biassed conclusions; experimental results should be comprehensively interpreted from both reaction kinetics and heat–mass transfer perspectives.

(6) When extrapolating pyrolysis findings from laboratory scale to in situ reservoir scale, the dominant change lies not in the pyrolysis reaction itself, but in the altered physical surrounding environment. Laboratory-scale experiments focus primarily on particle-level pyrolysis kinetics and product yields, whereas in situ pyrolysis additionally requires consideration of reservoir-scale heat transfer, fluid flow, hydrocarbon migration and pore fracture evolution. Therefore, future in situ pyrolysis simulations ought to couple kinetic models, temperature fields, species transport, multiphase flow and reservoir property evolution, so as to realize the transition from "kinetic parameter computation" to "reservoir-scale hydrocarbon production prediction".

**Author Contributions:** Conceptualization, Y.W. and Z.T.; methodology, Q.X.; software, M.Z.; validation, Z.W.; investigation, Z.W.; data curation, J.S.; writing—original draft preparation, J.S.; writing—review and editing, H.L.; project administration, Z.T. and Y.W. All authors have read and agreed to the published version of the manuscript.

**Funding:** National R&D Center for Oil Shale Extraction (Grant No. 33550000-24-ZC0613-0057).

**Data Availability Statement:** The original contributions presented in this study are included in the article. For further inquiries, please contact the corresponding author directly.

**Acknowledgments:** We would like to thank the National R&D Center for Oil Shale Extraction for their assistance.

**Conflicts of Interest:** Author Yuanqing Wang was employed by the Petroleum Exploration and Production Research Institute of SINOPEC company. The remaining authors declare that the research was conducted in the absence of any commercial or financial relationships that could be construed as a potential conflict of interest.

## References

1. Wang, S. Research Status on Mechanism of Oil Shale Pyrolysis. *J. Shanghai Univ. Eng. Sci.* **2016**, *30*, 209–213.
2. Dogan, M.; Uysal, B.Z. Non-isothermal pyrolysis kinetics of three Turkish oil shales. *Fuel* **1996**, *75*, 1424–1428. [CrossRef]
3. Khalil, A.M. Oil shale pyrolysis and effect of particle size on the composition of shale oil. *Oil Shale* **2013**, *30*, 138–146. [CrossRef]
4. Granoff, B.; Nuttall, H.E. Pyrolysis kinetics for oil-shale particles. *Fuel* **1977**, *56*, 234–240. [CrossRef]
5. Janković, B. The kinetic modeling of the non-isothermal pyrolysis of Brazilian oil shale: Application of the Weibull probability mixture model. *J. Pet. Sci. Eng.* **2013**, *111*, 25–36. [CrossRef]
6. Skala, D.; Kopsch, H.; Sokić, M.; Neumann, H.; Jovanović, J. Kinetics and modelling of oil shale pyrolysis. *Fuel* **1990**, *69*, 490–496. [CrossRef]
7. Yang, D.; Wang, L.; Zhao, Y.S.; Kang, Z. Investigating pilot test of oil shale pyrolysis and oil and gas upgrading by water vapor injection. *J. Pet. Sci. Eng.* **2021**, *196*, 108101. [CrossRef]
8. Li, D.; Pan, H.; Di, X.; Liu, X.; Hu, H. Progress in Catalytic Pyrolysis of Oil Shale. *Scanning* **2021**, *2021*, 6759176. [CrossRef]
9. Luo, X.; Hou, L.H.; Zhao, Z.Y.; Lin, S.H.; Pang, Z.L.; Zhang, L.J.; Han, W.X.; Li, Y. Exploitation and Utilization of Generated Oil and Gas by Pyrolysis Simulation Modeling of Shale Source Rocks Under the Condition of In Situ Conversion. *Processes* **2024**, *12*, 121. [CrossRef]
10. Moine, E.C.; Groune, K.; El Hamidi, A.; Khachani, M.; Halim, M.; Arsalane, S. Multistep process kinetics of the non-isothermal pyrolysis of Moroccan Rif oil shale. *Energy* **2016**, *115*, 931–941. [CrossRef]
11. Bai, F.; Sun, Y.; Liu, Y.; Li, Q.; Guo, M. Thermal and kinetic characteristics of pyrolysis and combustion of three oil shales. *Energy Convers. Manag.* **2015**, *97*, 374–381. [CrossRef]
12. Tiwari, P.; Deo, M. Detailed kinetic analysis of oil shale pyrolysis TGA data. *AIChE J.* **2012**, *58*, 505–515. [CrossRef]
13. Tiwari, P.; Deo, M. Compositional and kinetic analysis of oil shale pyrolysis using TGA-MS. *Fuel* **2012**, *94*, 333–341. [CrossRef]
14. Williams, P.T.; Ahmad, N. Investigation of oil-shale pyrolysis processing conditions using thermogravimetric analysis. *Appl. Energy* **2000**, *66*, 113–133. [CrossRef]
15. Wang, Y.W.; Wang, Y.P.; Meng, X.L.; Su, J.Z.; Long, Q.L. Organic matter pyrolysis kinetics and formation permeability variation during upgrading process of low-maturity shale oil. *Oil Gas. Geol.* **2019**, *40*, 678–684.
16. Li, Y.B.; Xue, L.F.; Ma, J.X. Numerical simulation of the changes of porosity and permeability in in-situ pyrolysis of oil shale. *Sci. Technol. Eng.* **2018**, *18*, 43–50.
17. Sun, X. Numerical Simulation of Hydrocarbon Generation Process in In-Situ Mining of Oil Shale. Master's Thesis, Jilin University, Changchun, China, 2019.

18. Le Doan, T.V.; Bostrom, N.W.; Burnham, A.K.; Kleinberg, R.L.; Pomerantz, A.E.; Allix, P. Green River Oil Shale Pyrolysis: Semi-Open Conditions. *Energy Fuels* **2013**, *27*, 6447–6459. [CrossRef]
19. Hillier, J.L.; Fletcher, T.H. Pyrolysis Kinetics of a Green River Oil Shale Using a Pressurized TGA. *Energy Fuels* **2011**, *25*, 232–239. [CrossRef]
20. Kuang, W.Q.; Lv, M.K.; Yeboah, I.; Qian, G.; Duan, X.Z.; Yang, J.; Chen, D.; Zhou, X.G. A comprehensive kinetics study on non-isothermal pyrolysis of kerogen from Green River oil shale. *Chem. Eng. J.* **2019**, *377*, 120275. [CrossRef]
21. He, L.; Ma, Y.; Yue, C.T.; Wu, J.X.; Li, S.Y. Kinetic modeling of Kukersite oil shale pyrolysis with thermal bitumen as an intermediate. *Fuel* **2020**, *279*, 118371. [CrossRef]
22. Lu, H.; Pan, H.D.; Guo, C.; Liu, X.Y.; Wang, C.H.; Yue, Y. Comparative study on pyrolysis kinetic model of Fushun oil shale. *J. Liaoning Shihua Univ.* **2020**, *40*, 20–26.
23. Pan, N.; Li, D.; Lü, W.; Dai, F.Q. Kinetic study on the pyrolysis behavior of Jimsar oil shale. *Oil Shale* **2019**, *36*, 462–482. [CrossRef]
24. Dong, F.K.; Cao, L.; Zhang, J. Study on pyrolysis and kinetic model of Jimsar oil shale. *Petrochem. Ind. Appl.* **2019**, *38*, 29–34.
25. Hua, Z.J.; Wang, Q.; Jia, C.X.; Liu, Q. Pyrolysis kinetics of a Wangqing oil shale using thermogravimetric analysis. *Energy Sci. Eng.* **2019**, *7*, 912–920. [CrossRef]
26. Xue, H.Q.; Li, S.Y.; Wang, H.Y.; Zheng, D.W.; Fang, C.H. Pyrolysis kinetics of oil shale from northern Songliao Basin in China. *Oil Shale* **2010**, *27*, 5–16. [CrossRef]
27. Moine, E.C.; Bouamoud, R.; El Hamidi, A.; Khachani, M.; Halim, M.; Arsalane, S. Mineralogical characterization and non-isothermal pyrolysis kinetics of Moroccan Rif oil shale. *J. Therm. Anal. Calorim.* **2017**, *131*, 993–1004. [CrossRef]
28. Abu El-Rub, Z.; Kujawa, J.; Al-Gharabli, S. Pyrolysis Kinetic Parameters of Omari Oil Shale Using Thermogravimetric Analysis. *Energies* **2020**, *13*, 4060. [CrossRef]
29. Jaber, J.O.; Probert, S.D. Pyrolysis and gasification kinetics of Jordanian oil-shales. *Appl. Energy* **1999**, *63*, 269–286. [CrossRef]
30. Bouamoud, R.; Moine, E.C.; Mulongo-Masamba, R.; El Hamidi, A.; Halim, M.; Arsalane, S. Type I kerogen-rich oil shale from the Democratic Republic of the Congo: Mineralogical description and pyrolysis kinetics. *Pet. Sci.* **2020**, *17*, 255–267. [CrossRef]
31. Wang, W.; Li, S.Y.; Li, L.Y.; Ma, Y.; Yue, C.T.; He, J.L. Pyrolysis Kinetics of North-Korean Oil Shale. *Oil Shale* **2014**, *31*, 250–265. [CrossRef]
32. Wang, W.; Li, S.Y.; Yue, C.T.; Ma, Y. Multistep pyrolysis kinetics of North Korean oil shale. *J. Therm. Anal. Calorim.* **2015**, *119*, 643–649. [CrossRef]
33. Cao, R.; Yang, D.; Kang, Z.; Huang, D.; Cui, Z.; Lu, Y. Effects of Inherent Minerals on Pyrolysis Behavior and Kinetics of Jimsar Oil Shale. *ACS Omega* **2023**, *8*, 40396–40406. [CrossRef]
34. Jiang, H.; Song, L.; Cheng, Z.; Chen, J.; Zhang, L.; Zhang, M.; Hu, M.; Li, J.; Li, J. Influence of pyrolysis condition and transition metal salt on the product yield and characterization via Huadian oil shale pyrolysis. *J. Anal. Appl. Pyrolysis* **2015**, *112*, 230–236. [CrossRef]
35. Yu, M.Y.; Zhan, J.H. Research Progress in Mechanism of Oil Shale Pyrolysis. *Liaoning Chem. Ind.* **2024**, *53*, 579–582.
36. Bai, F.; Sun, Y.; Liu, Y.; Guo, M. Evaluation of the porous structure of Huadian oil shale during pyrolysis using multiple approaches. *Fuel* **2017**, *187*, 1–8. [CrossRef]
37. Saif, T.; Lin, Q.Y.; Bijeljic, B.; Blunt, M.J. Microstructural imaging and characterization of oil shale before and after pyrolysis. *Fuel* **2017**, *197*, 562–574. [CrossRef]
38. Xi, Y.; Li, J.; Lian, W.; Fu, H.F.; Qi, Y.; Tian, Y.D. Research on the Pore Evolution of Oil Shale under Different Thermal Treatment Temperatures Using NMR and FESEM Methods. *Geofluids* **2023**, *2023*, 6101374. [CrossRef]
39. Liu, Z.J.; Ma, H.T.; Guo, J.P.; Liu, G.; Wang, Z.; Guo, Y.Z. Pyrolysis Characteristics and Effect on Pore Structure of Jimsar Oil Shale Based on TG-FTIR-MS Analysis. *Geofluids* **2022**, *2022*, 7857239. [CrossRef]
40. Tang, Y.L.; Wu, H.; Yan, Y.L.; Pan, H.D.; Zhao, L.; Ma, H.F.; Hu, Z.Y. Research Progress in the Pyrolysis Technology of Oil Shale. *Liaoning Chem. Ind.* **2022**, *51*, 1094–1097.
41. Li, Y.Y.; Li, J.; Zhou, S.X.; Meng, B.K.; Wu, T. A review on thermogravimetric analysis-based analyses of the pyrolysis kinetics of oil shale and coal. *Energy Sci. Eng.* **2024**, *12*, 329–355. [CrossRef]
42. Li, L.L.; Zhang, F.Q. Analysis of Factors Affecting Pyrolysis of Oil Shale. *Liaoning Chem. Ind.* **2023**, *52*, 1012–1016. [CrossRef]
43. Li, T.Z. Analysis of Oil Shale Low-temperature Pyrolysis Process and its Influencing Factors. *Shanxi Chem. Ind.* **2023**, *212*, 74–76.
44. Xu, J.Z.; Chen, Z.X.; Zhou, D.S.; Nie, W.C.; Li, R. Review on the Characteristics of Pyrolysis During In-situ Conversion of Oil Shale. *J. Southwest Pet. Univ. (Sci. Technol. Ed.)* **2021**, *43*, 220–226.
45. Li, Y. Research on In Situ Exploitation Method and Well Pattern Optimization of Oil Shale in Block A of Jilin Oilfield. Master's Thesis, China University of Geosciences (Beijing), Beijing, China, 2021.
46. Wang, E.N. Numerical Simulation Study on Large-Scale In-Situ Exploitation of Oil Shale. Ph.D. Thesis, Jilin University, Changchun, China, 2023.
47. Li, Z. Numerical Simulation of Oil Shale In-Situ Upgrading by Steam Injection. Master's Thesis, China University of Petroleum (East China), Qingdao, China, 2017.

48. Liu, X. Numerical Simulation of Heat Transfer Characteristics of Oil Shale in High Temperature Supercritical Carbon Dioxide Mining. Ph.D. Thesis, China University of Petroleum (Beijing), Beijing, China, 2021.
49. Dong, F.K. Study on the Law of Pollutant Migration During In-Situ Heat Injection to Exploit Oil Shale. Ph.D. Thesis, Taiyuan University of Technology, Taiyuan, China, 2019.
50. Wu, M. The Study of Electric Heating on Hydrocarbon Generation and Pores Evolution of Shale in North Songliao Basin. Master's Thesis, China University of Petroleum (East China), Qingdao, China, 2020.
51. Bai, F.T. Theoretical and Experimental Research of Oil Shale Pyrolysis Triggered by Topochemical Heat. Ph.D. Thesis, Jilin University, Changchun, China, 2015.
52. Dong, G.S. Research on the Optimization and Regulation of Oil Shale Autogenous Thermal In-Situ Transformation with High Efficiency. Ph.D. Thesis, Jilin University, Changchun, China, 2024.
53. Yang, L.H.; Zhu, C.F.; Zeng, H.; Su, J.Z.; Wang, Y.W.; Wu, J.W.; Chen, X.D.; Guo, W. Numerical simulation analysis on the development effect of vertical well and horizontal well during oil shale autothermic pyrolysis in-situ conversion process: A case study of oil shale in Xunyi area, Ordos Basin. *Acta Pet. Sin.* **2023**, *44*, 1333–1343.
54. Raja, M.A.; Zhao, Y.S.; Zhang, X.P.; Li, C.S.; Zhang, S.J. Practices for modeling oil shale pyrolysis and kinetics. *Rev. Chem. Eng.* **2018**, *34*, 21–42. [CrossRef]
55. Kök, M.V.; Pamir, R. Pyrolysis kinetics of oil shales determined by DSC and TG/DTG. *Oil Shale* **2003**, *20*, 55–66. [CrossRef]
56. Lü, X.S.; Sun, Y.H.; Lu, T.; Bai, F.T.; Viljanen, M. An efficient and general analytical approach to modelling pyrolysis kinetics of oil shale. *Fuel* **2014**, *135*, 182–187. [CrossRef]
57. Li, S.Y.; Yue, C.T. Study of different kinetic models for oil shale pyrolysis. *Fuel Process. Technol.* **2003**, *85*, 51–61. [CrossRef]
58. Li, S.Y.; Yue, C.T. Study of pyrolysis kinetics of oil shale. *Fuel* **2003**, *82*, 337–342. [CrossRef]
59. Ma, Y.; Li, S.Y. The mechanism and kinetics of oil shale pyrolysis in the presence of water. *Carbon Resour. Convers.* **2018**, *1*, 160–164. [CrossRef]
60. Wang, Z.J.; Deng, S.H.; Gu, Q.; Zhang, Y.M.; Cui, X.J.; Wang, H.Y. Pyrolysis kinetic study of Huadian oil shale, spent oil shale and their mixtures by thermogravimetric analysis. *Fuel Process. Technol.* **2013**, *110*, 103–108. [CrossRef]
61. Zhang, J.; Ding, Y.; Du, W.; Lu, K.; Sun, L. Study on pyrolysis kinetics and reaction mechanism of Beizao oil shale. *Fuel* **2021**, *296*, 120696. [CrossRef]
62. Zhao, S.; Sun, Y.H.; Lü, X.S.; Li, Q. Kinetics and thermodynamics evaluation of carbon dioxide enhanced oil shale pyrolysis. *Sci. Rep.* **2021**, *11*, 516. [CrossRef]
63. Zhang, J.J.; Zhang, F.Q.; Han, J.T. Study on Pyrolysis Characteristics of Oil Shale. *Liaoning Chem. Ind.* **2019**, *48*, 757–759.
64. Al-Ayed, O.S.; Matouq, M.; Anbar, Z.; Khaleel, A.M.; Abu-Nameh, E. Oil shale pyrolysis kinetics and variable activation energy principle. *Appl. Energy* **2010**, *87*, 1269–1272. [CrossRef]
65. Al-Harahsheh, M.; Al-Ayed, O.; Robinson, J.; Kingman, S.; Al-Harahsheh, A.; Tarawneh, K.; Saeid, A.; Barranco, R. Effect of demineralization and heating rate on the pyrolysis kinetics of Jordanian oil shales. *Fuel Process. Technol.* **2011**, *92*, 1805–1811. [CrossRef]
66. Jiang, X.M.; Han, X.X.; Cui, Z.G. Mechanism and Mathematical Model of Huadian Oil Shale Pyrolysis. *J. Therm. Anal. Calorim.* **2006**, *86*, 457–462. [CrossRef]
67. Zhang, X. Research on Oil Shale In-Situ Pyrolysis Characteristics and Mechanism Under High-Pressure Conditions. Ph.D. Thesis, Jilin University, Changchun, China, 2024.
68. Wang, G.Y. Evolution of Anisotropic Thermophysical, Hydraulic, Mechanical Characteristics Under High Temperature and Its Application. Ph.D. Thesis, Taiyuan University of Technology, Taiyuan, China, 2019.
69. Ma, W.L. Study on the Evolution Laws of Structural and Mechanical Characteristics of Oil Shale During Temperature Rise and the Application of Numerical Simulation. Ph.D. Thesis, Jilin University, Changchun, China, 2022.
70. Tang, J.P.; Yu, H.H. Research status and prospect on physical simulation test of oil shale in-situ mining. *J. Liaoning Tech. Univ. (Nat. Sci.)* **2024**, *43*, 565–580.
71. Wang, E.N.; Xue, L.F.; Zhang, X.Y.; Li, Y.B. Numerical Simulation Study of Large-scale in-situ Exploitation of Oil Shale and Discussion of Production Parameters. *Coal Geol. China* **2023**, *35*, 20–28.
72. Zheng, S.J. Study on the Characteristics of Temperature Distribution and Its Influence on the In-Situ Heating Process for Oil Shale. Master's Thesis, Northeast Petroleum University, Daqing, China, 2023.
73. Wang, J. Experimental Study on In-Situ Pyrolysis of Oil Shale. Master's Thesis, Xi'an Shiyou University, Xi'an, China, 2021.
74. Liu, S. Numerical Simulation of In-Situ Pyrolysis of Oil Shale. Master's Thesis, Xi'an Shiyou University, Xi'an, China, 2023.


**Disclaimer/Publisher's Note:** The statements, opinions and data contained in all publications are solely those of the individual author(s) and contributor(s) and not of MDPI and/or the editor(s). MDPI and/or the editor(s) disclaim responsibility for any injury to people or property resulting from any ideas, methods, instructions or products referred to in the content.